MLCV Coursework 2 Report

Shinyoung Yu
20200405
School of Computing
sahaa0918@kaist.ac.kr

Jiyun Park
20210263
School of Computing
jiyun02@kaist.ac.kr

1. K-means codebook

We implemented the classification process following the visual codebook pipeline provided in the instruction. First, we extracted 100K SIFT feature descriptors from the training data and applied K-means clustering to construct a visual vocabulary.

1.1. Vocabulary size of K-means clustering

Theoretically, a smaller visual vocabulary size K increases the risk of underfitting but offers better time-wise efficiency. Conversely, a larger K poses a higher risk of overfitting and results in lower efficiency. Theoretically, the time complexity of K-means clustering training and vector quantization is proportional to the value of K, and our result Fig. 1 align with it.

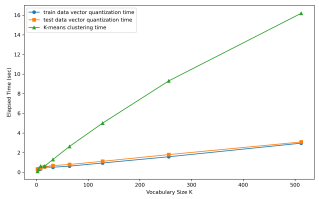

Figure 1. K-means visual vocabulary: training and quantization time according to the value of k

1.2. Vector quantisation process

To quantize images, the SIFT feature descriptors extracted from each image were assigned to the nearest vocabulary cluster, and a histogram vector was generated based on the vocabulary frequency of such assigning result. Consequently, after vector quantization, the dimension of each image was reduced to the size of visual vocabulary, denoted by K.

2. Incremental PCA

2.1. Important parameter in implementation: d_3

To implement incremental PCA, we utilized the algorithm from the "Online Learning" slides presented in class. Here, a key parameter is d_2 and d_3. When new data arrives in incremental PCA, computing the eigenspace model for this subset requires $O(\min(D, N')^3)$ time, where N' is the number of data points in the subset. Additionally, merging this new eigenspace model with the existing data takes $O((d_1 + d_2 + 1)^3)$ time, where d_1 is equal to the previously computed eigenspace model's d_3 value. Therefore, to enhance time efficiency in incremental PCA, it is essential to keep d_3 small, although this results in a time-accuracy tradeoff by dropping less-significant eigenvector information, which is represented by our experiment result Fig. 2

Figure 2. Incremental PCA's time-accuracy tradeoff according to the value of d_3

2.2. Comparison with other PCA

We compared the results of each incremental PCA stage (i.e.adding training data in four batches) with the results of batch PCA in the following four aspects. In summary, incremental PCA is a good approximation of batch PCA, and even requires less training time.

- Training time: For batch PCA, we measured training time by re-training the model each time new data was added. The results are shown in Fig. 3a. Using one subset, the training time is approximately the same for both methods. However, as we add more data, the value of N increases for batch PCA, while the values of N' and d_3 remain constant for incremental PCA, maintaining constant time and improving time-wise efficiency.
- Accuracy of incremental PCA: In incremental PCA, time-accuracy tradeoff occurs since less-significant eigenvec-

tors are dropped during $d_1 + d_2$ merging, retaining only the top d_3 eigenvectors. We calculated the cosine similarity of eigenvectors, eigenvalues, and mean vectors between incremental PCA at each stage and batch PCA calculated by corresponding data, as shown in Fig. 3b. As more training data is added, the number of discarded less-significant eigenvectors increases, resulting in decreased similarity between eigenvectors; the similarity after adding the last subset is 0.856. For mean vectors and eigenvalues, cosine similarities are 1 and close to 1 respectively, indicating that the incremental PCA is a good approximation.

- Reconstruction error: Referring to Fig. 3c, the reconstruction error for incremental PCA using all training data (i.e., after adding the 4th batch) is almost identical to that of batch PCA with the same amount of data. This also demonstrates that incremental PCA gives similar result to batch PCA.
- Face recognition accuracy: In the optimal settings of batch PCA found in Question1 (i.e. K=1 and bases=90) the accuracy ranks as follows: full-data batch PCA > full-data incremental PCA > PCA using only the first training set. This indicates that classification accuracy improves progressively with the increase in training data. Additionally, using incremental PCA in place of batch PCA results in an accuracy drop of approximately 6.67%, also indicating a time-accuracy tradeoff.

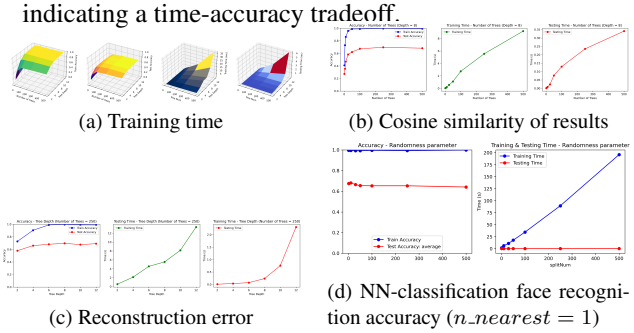

(a) Training time (b) Cosine similarity of results

(c) Reconstruction error (d) NN-classification face recognition accuracy ($n\_nearest = 1$)

Figure 3. Comparison between Incremental and Batch PCA methods

3. LDA Ensemble for Face Recognition

PCA can effectively reduce the dimension of input data preserving important features. And LDA can maximize the variance of between-class while minimize between-class. Thus, using PCA-LDA is expected to increase computing efficiency and classification accuracy. In this section, we try to figure out the effect of PCA-LDA via some experiments.

3.1. Recognition accuracy of PCA-LDA

To implement PCA-LDA, we set M_{pca} and M_{lda} by measuring classification accuracy with M_{pca} from 1 to 415 and M_{lda} from 1 to $min(M_{pca} - 1, 51)$. This is because, the maximum possible projection dimension for PCA is $N - 1$ since the total number of principal components can not be larger than overall data, and for LDA is $n_{class} - 1$ since the number of direction for maximizing the distance of between-class and minimizing within-class cannot be larger than the total number of classes. As shown in Fig. 4, accuracy peaked at $M_{pca} = 150$ and $M_{lda} = 50$. Higher M_{lda} improves performance by enhancing data discrimination, while optimal M_{pca} is between 100 and 200, balancing information retention and overfitting risk.

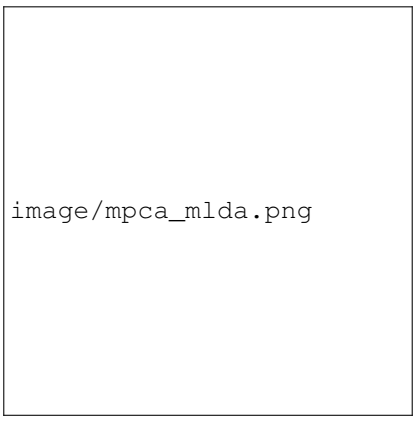

Figure 4. Classification accuracy varying Mpca and Mlda

In LDA, the rank of within-class scatter matrix(S_w) is $min(364, M_{pca})$, where $N - n_{class} = 416 - 52 = 364$ and the rank of between-class scatter matrix(S_b) is $n_{class} - 1 = 51$. Since $\sum_{x \in D_i}(x - m_i) = 0$, each class is linearly dependent, so, $S_w = \sum_{i=1}^{c} \sum_{x \in D_i}(x - m_i)(x - m_i)^T$ has at most $N - n_{class}$ linearly independent row vectors. After reducing dimensions using PCA, the rank of S_w cannot exceed M_{pca} as the vectors are confined to the PCA subspace. For S_b defined as $S_b = \sum_{i=1}^{c}(m_i - m)(m_i - m)^T$, it depends only ionly on class means, and since their relationship of class mean does not change after PCA projection since their relationships remain unchanged under PCA (a linear transformation), the maximum possible rank for S_b is $N - n_{class}$.

Based on this observation, we decided to fix $M_{pca} = 150$ and $M_{lda} = 50$ for future experiments. Detailed result including confusion matrix and images can be found in Appendix B and Appendix C.

3.2. PCA-LDA Ensemble

There are 3 hyperparameter that we can handle randomness: the number of random vector in feature space, the proportion of training data for subsampling, and the number of models for the ensemble. We will examine the impact of each one one by one.

First, we look into randomization in feature space($M1$). As Fig. 5a indicates, the accuracy is almost highest when the number of random samples is around 30. This is because if the number of random vectors is too large, impor-

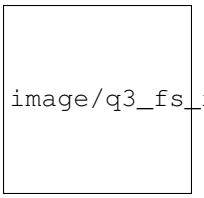

(a) Randomization in feature space

(b) Random data subsampling

(c) randomization in the number of base-models

Figure 5. Accuracy comparison between randomness parameters

tant features cannot be preserved. However if it is too small, since each base model become more similar, the advantages of ensembling is diminished. Therefore, it is estimated that optimization occurred when the number of random vectors was 30.

Next, we observe the impact of data subsampling proportion(α). Fig. 5b shows that the more data we use, slightly better accuracy we get. Since the number of training data is small, the benefit of generalizing each model outweighs the benefit gained from randomness.

Lastly, regarding the effect of the number of base models(n_{model}), we varied the number from 1 to 60, as shown in Fig. 5c. When there are fewer than 30 models, the results are similar to a single PCA-LDA model. However, with more than 30 models, performance improves significantly, though further increases beyond 30 yield minimal gains. This is because up to 30 models, the ensemble can capture diverse features for generalization, but the PCA-LDA model's limited ability to capture complex patterns prevents substantial improvement beyond that point. We used "majority voting" for combining predictions, as it's most suitable for classification tasks where each class lacks numeric meaning, making it more appropriate than methods like averaging or maximum selection.

Considering both accuracy and computation cost, we conclude that the ensemble model with $M1 = 30$, $\alpha = 0.9$, $n_{model} = 30$ has the best performance.

3.3. Result of PCA-LDA Ensemble

The accuracy of committee machine, which gather all prediction results from each base models from ensemble model, is 0.846. And the average of individual models in ensemble model is 0.736. From this result, we can check that the performance of committee machine is better than individual as we learned. (Ensemble Learning LN, p.11-13)

In addition, by comparing the number of off-diagonal components of confusion matrices, (Fig. 7b and Fig. 7c) we can visually check that the performance of ensemble model is better.

4. Generative and Discriminative Subspace Learning

PCA is a generative model, which aims to reconstruct the input. And LDA is a discriminative model, which conducts classification. If we want to take advantages of both methods, it is inevitable to redisign the objective function.

4.1. Objective function

To achieve our goal, it is natural to think of a function that combine objective functions of PCA and LDA.

Eq. (1) is identical to PCA objective function when $\alpha = 1$ and to LDA objective function when $\alpha = 0$. Our goal is to find W that maximizes $J(W)$ since reconstruction error is reduced and subspaces become more discriminative when PCA, LDA objective functions are maximized. Such W must satisfy Eq. (2) for some constant λ.

$$J(W) = \alpha W^T S W + (1-\alpha)\frac{W^T S_b W}{W^T S_w W} \tag{1}$$

$$(\alpha S + (1-\alpha)S_b)W = \lambda(\alpha I + (1-\alpha)S_w)W \tag{2}$$

If $\alpha I + (1-\alpha)S_w$ is invertible, we can easily get W using eigenvector-eigenvalue method. Using this method, we can reduce computation time and memory space required to store the train parameters since we only use one weignt matrix W. However, it is more difficult to visualize the result of feature extraction of PCA compared to PCA-LDA's sequential data transformation. Detailed derivation and the pros/cons of this method can be found in Appendix D.

Appendix

A. Q1: Mean face

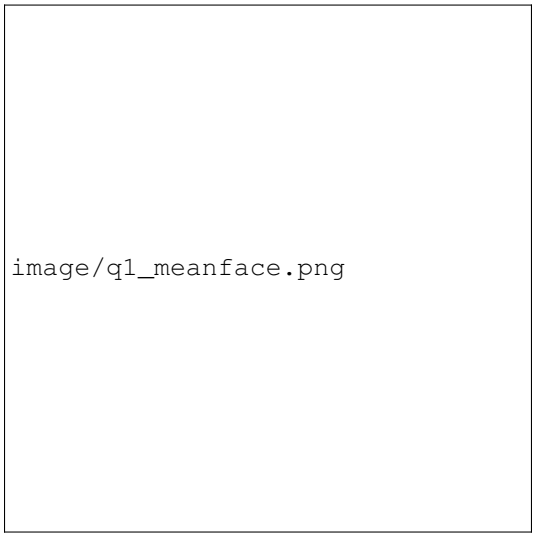

Figure 6. Mean face of training data

B. Q1,3: Confusion matrix

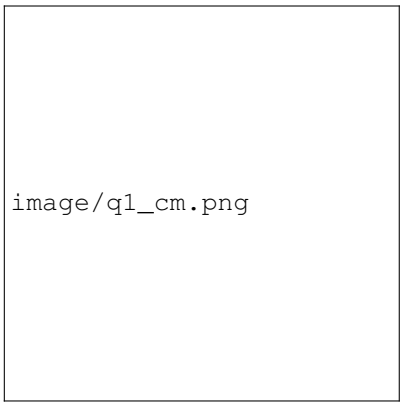

(a) Confusion matrix of PCA

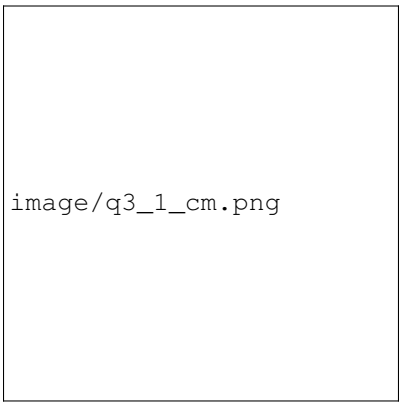

(b) Confusion matrix of PCA-LDA

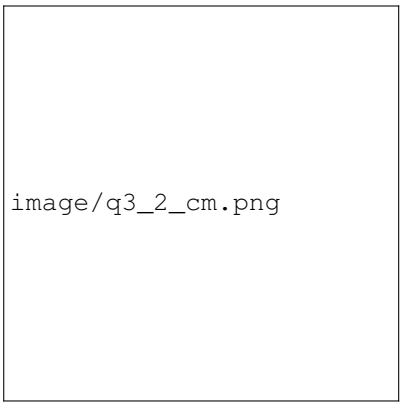

(c) Confusion matrix of Emsenble model

Figure 7. Confusion matrix of PCA, PCA-LDA, and PCA-LDA ensemble model

As shown in Fig. 7, confusion matrix of PCA has much more off-diagonal elements than PCA-LDA and Ensemble model. This shows that the prediction is much more successful using PCA-LDA and Ensemble model than PCA. Also, Ensemble model has slightly less off-diagonal elements than PCA-LDA. This indicates Ensemble model is more accurate in classification than the original model.

C. Q1,3: Prediction examples

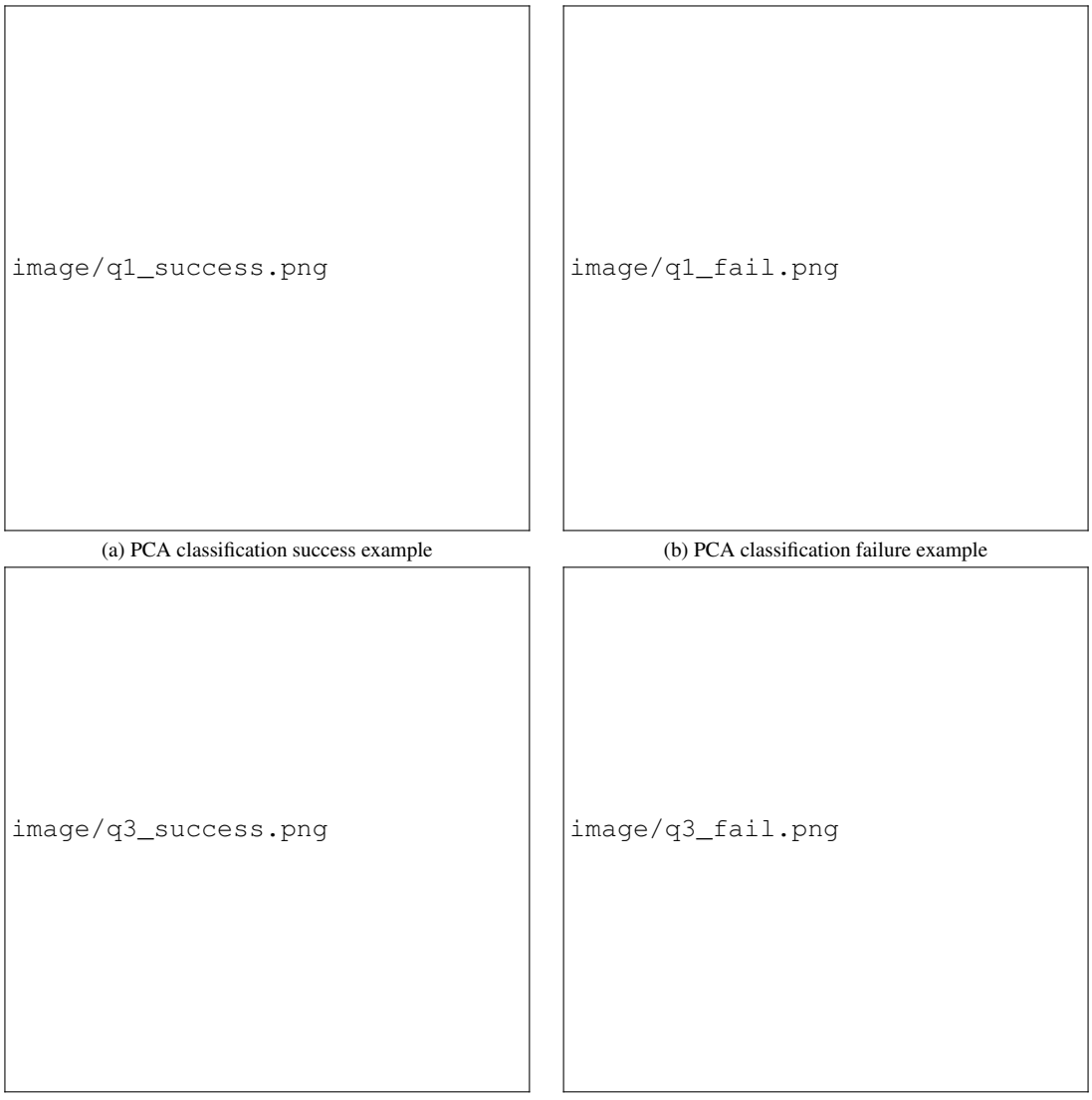

(a) PCA classification success example

(b) PCA classification failure example

(c) PCA-LDA classification success example

(d) PCA-LDA classification failure example

Figure 8. The success/failuer examples of PCA and PCA-LDA with NN classification

Above images shows successful and failure examples of classification using PCA and PCA-LDA. If we take a closer look at successful cases, the model infer the class accurately despite different angles of face. This may because the model can generalize well across different angles of the face. For failure cases, the prediction appears to have failed because the glasses and facial expressions are similar.

D. Q4: Generative and Discriminative Subspace Learning

Below is the objective function for generative and discriminative subspace learning. Our goal is to find W that maximizes $J(W)$

$$J(W) = \alpha W^T S W + (1-\alpha)\frac{W^T S_b W}{W^T S_w W} \tag{3}$$

Eq. (3) can be changed as Eq. (4) since $W^TW = I$. (This is because, W is a projection matrix, hence W^TW indicates re-projection after projection to the subspace. Therefore, projected vector returns to itself after applying W^TW.)

$$J(W) = \alpha\frac{W^TSW}{W^TW} + (1-\alpha)\frac{W^TS_bW}{W^TS_wW} = \frac{W^T(\alpha S + (1-\alpha)S_b)W}{W^T(\alpha I + (1-\alpha)S_w)W} \tag{4}$$

If we keep the denominator constant, the problem we have to solve changes to the problem to maximize the numerator. Let the denominator $k(constant)$ and use Lagrange-multiplier. (Eq. (5))

$$W^T(\alpha I + (1-\alpha)S_w)W = k \tag{5}$$

$$L(W,\lambda) = W^T(\alpha S + (1-\alpha)S_b)W + \lambda(k - W^T\alpha I + (1-\alpha)S_w)W) \tag{6}$$

To get the solution, each partial derivatives of $L(W,\lambda)$ with respect to W and λ must be 0.

$$\frac{\partial L}{\partial W} = 2 * W(\alpha S + (1-\alpha)S_b - \lambda(\alpha I + (1-\alpha)S_w)) = 0 \tag{7}$$

$$\frac{\partial L}{\partial \lambda} = k - W^T(\alpha I + (1-\alpha)S_w)W = 0 \tag{8}$$

Eq. (8) is satisfied from our assumption of the denominator. Now, the only thing we have to consider is Eq. (7). If we organize Eq. (7), we can get Eq. (9).

$$(\alpha S + (1-\alpha)S_b)W = \lambda(\alpha I + (1-\alpha)S_w)W \tag{9}$$

If $\alpha I + (1-\alpha)S_w$ is invertible, the equation becomes as below.(Eq. (10))

$$(\alpha I + (1-\alpha)S_w)^{-1}(\alpha S + (1-\alpha)S_b)W = \lambda W \tag{10}$$

Since λ is some constants, we can regard Eq. (10) as a eigenvector-eigenvalue problem where W is an eigenvector matrix and lambda is an eigenvalue matrix.

We can discuss the foreseeable behavior when applying the resulting W matrix from the above equation to data. Since this optimization involves both PCA and LDA, it can blend the advantages of both methods, generating high-accuracy classification results similar to Question 3's PCA-LDA method.

The pros and cons of this approach are as follows: In Question 3, we trained W_{pca} and W_{lda} separately for PCA and LDA and used $W_{opt}^T = W_{lda}^TW_{pca}^T$. This requires solving two eigenvector-eigenvalue problems to derive each of W_{pca} and W_{lda}. However, by using our new objective function, we only need to solve one eigenvector-eigenvalue problem and store just the W matrix, which reduces both time complexity and the space required to store the trained parameters.

There are also some drawbacks to this approach. Simultaneously tuning the hyperparameters, α and the final dimension D (where $W = (N \cdot D)$), may be challenging. In Question 3, since we trained W_{pca} and W_{lda} separately, we could verify the effectiveness of PCA and LDA process individually by applying it step-by-step to real images and printing intermediate outputs (e.g., displaying the PCA-reconstructed image). However, in the method proposed for Question 4, such verification is not possible. In other words, if the current test accuracy is not high enough, it would be difficult to determine whether the issue arose during the PCA or LDA phase.

E. Q5: Test result's confusion matrix and success/failure cases

The optimal parameters determined for the random forest through experiments are $N = 250$, $D = 8$, and splitnum $= 10$. With this configuration, each real-time executable weak learner—axis-aligned and two-pixel tests—each was trained 10 times. The confusion matrix results in Fig. 9 represent the best test accuracy among the 10 repetitive train results.

Additionally, the example success and failure cases based on the confusion matrix results above are shown in Fig. 10, Fig. 11, Fig. 12, Fig. 13. Compared to the success cases, the failure cases show a higher similarity between the failed image and the predicted class, meaning that our model is reasonable.

F. Q5: Visualization of random forest's information gain process

Random forests utilize the entropy-based information gain method to reduce the diversity of classes within the nodes as they move down to the lower nodes. To illustrate the execution of this algorithm in our code, we have traced the path down the left child nodes of a single tree and represented the results in the histograms below. Each histogram corresponds to the left node of the previous figure, and the result Fig. 14 align with our expectations.

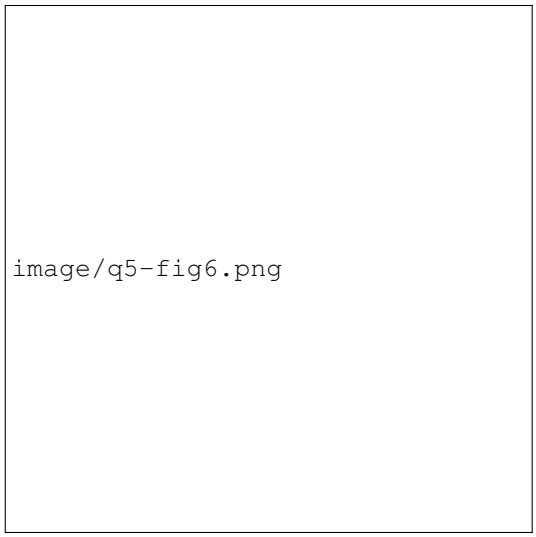

(a) Axis-aligned weak learner, test accuracy=0.644

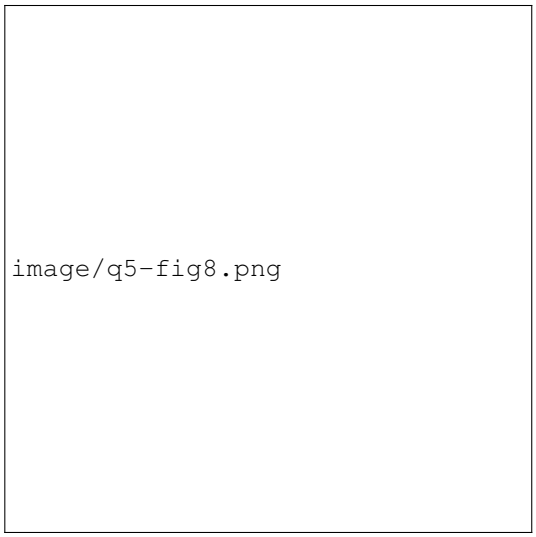

(b) Two-pixel test weak learner, test accuracy=0.692

Figure 9. Confusion matrix of optimal cases ($N = 250$, $D = 8$, and splitnum $= 10$)

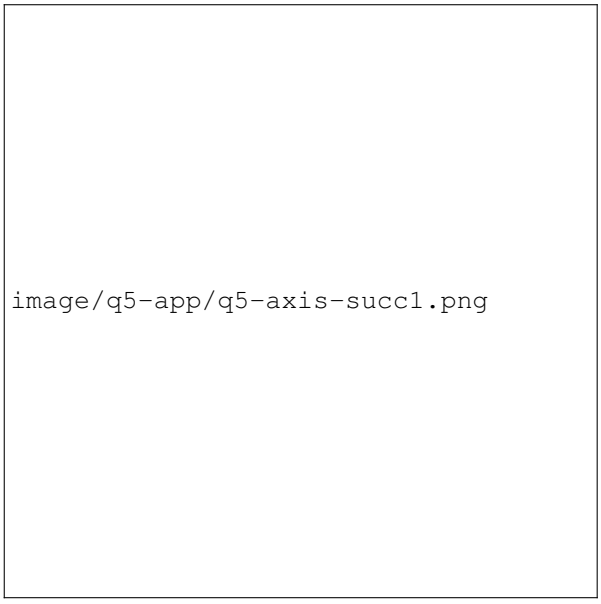

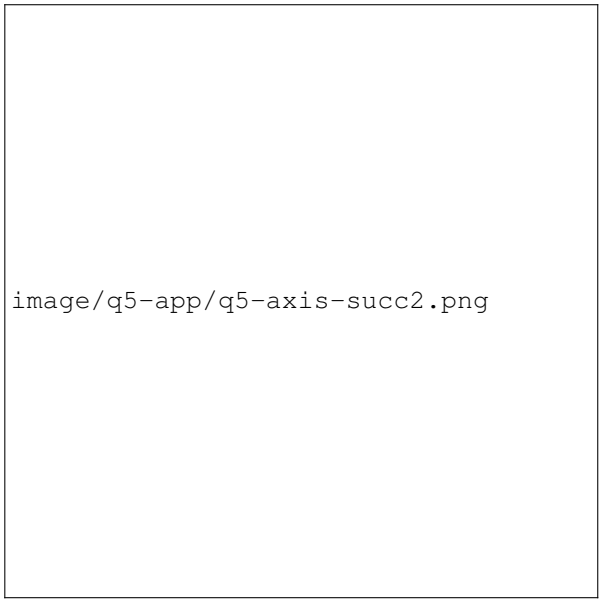

Figure 10. Axis-aligned weak learner: Example success case

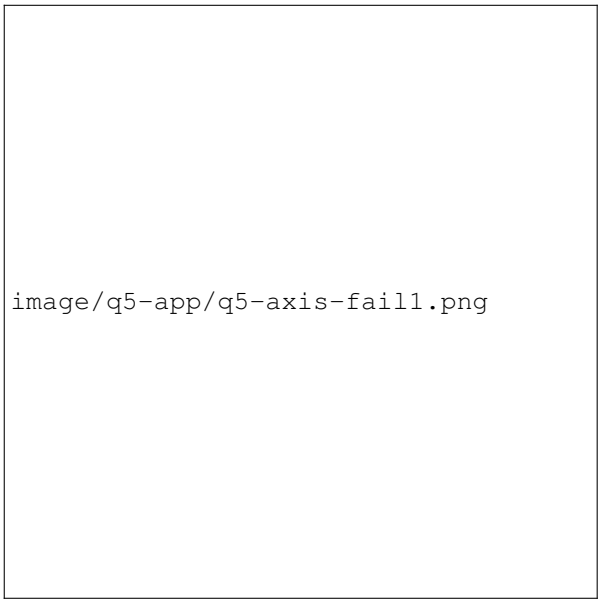

Figure 11. Axis-aligned weak learner: Example failure case

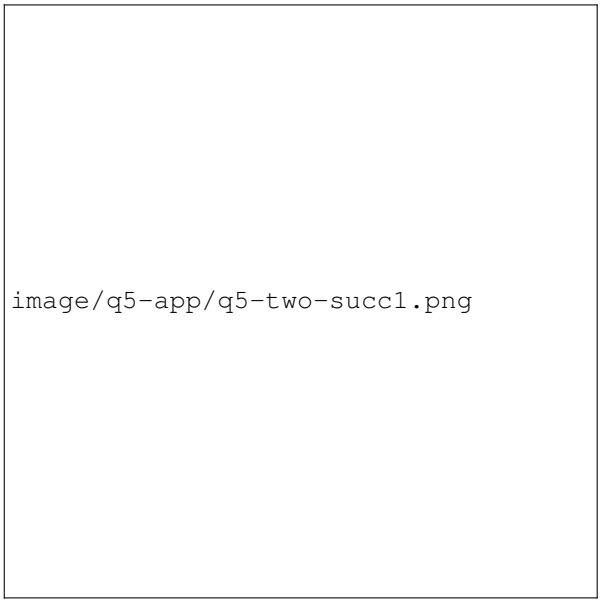

Figure 12. Two-pixel test weak learner: Example success case

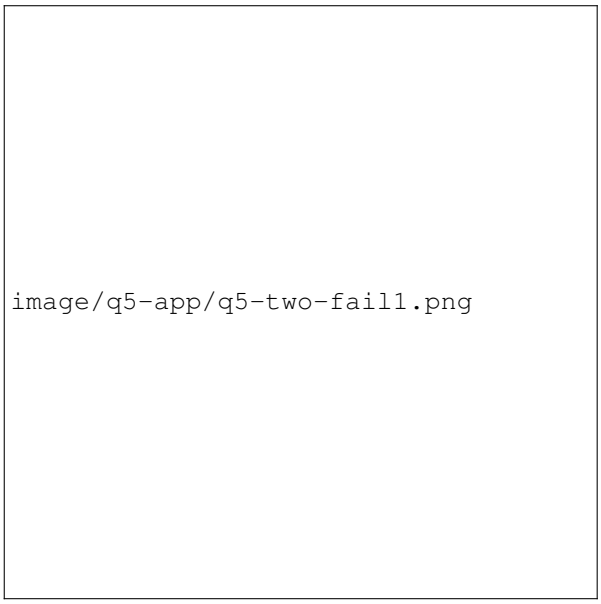

Figure 13. Two-pixel test weak learner: Example failure case

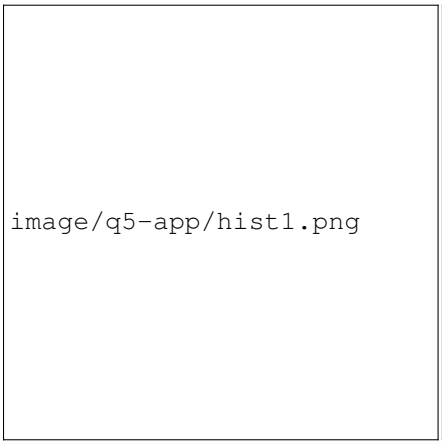

(a) Top node (depth=1)

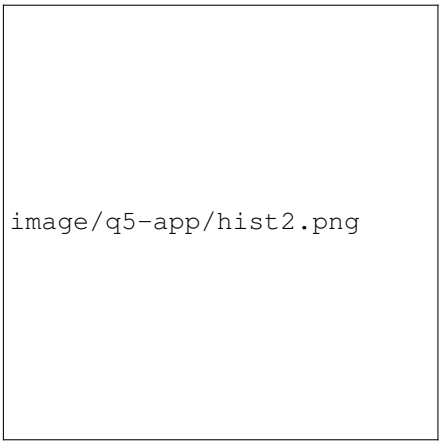

(b) depth=2

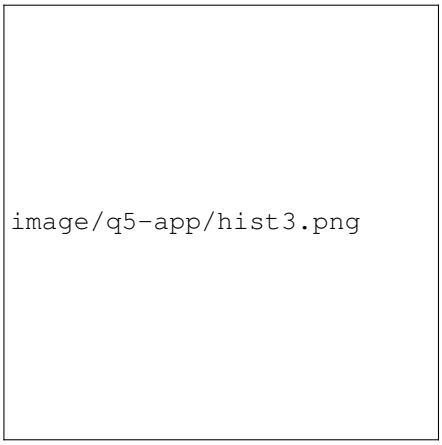

(c) depth=3

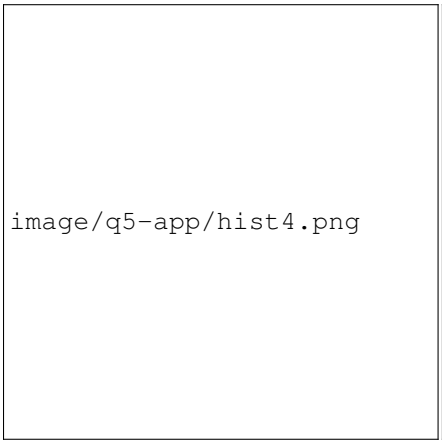

(d) depth=4

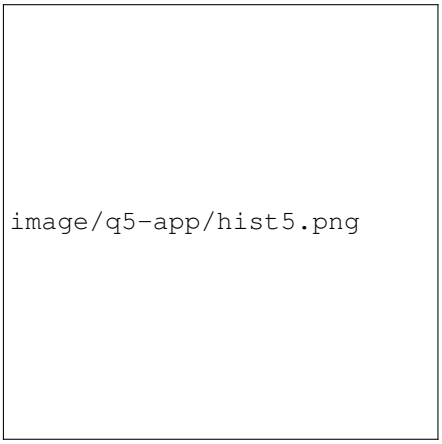

(e) depth=5

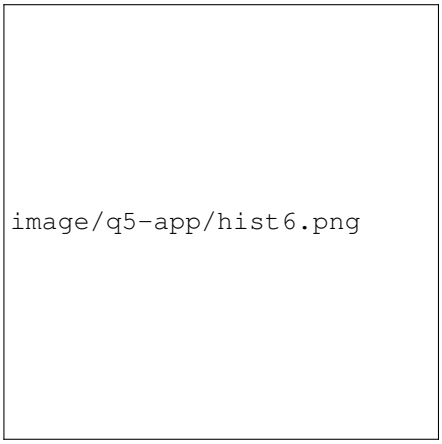

(f) Leaf (depth=6)

Figure 14. Visualization of random forest's information gain process